Dynamics of Free Dual-spin Spacecraft

Vladimir Aslanov

Abstract – This paper presents the study of the axial dual-spin spacecraft dynamics. These spacecraft are usually called gyrostats. The gyrostat is composed of two rigid bodies: an asymmetric platform and an axisymmetric rotor aligned with the platform principal axis. The dynamics of gyrostats without external torque is considered. The dynamics is described by using ordinary differential equations with Andoyer-Deprit canonical variables. For undisturbed motion, when the internal torque is equal to zero and the moments of inertia of the gyrostat are constant, the stationary solutions are found, and their stability is studied. Also we obtain general exact analytical solutions in terms of elliptic functions. These results can be interpreted as the development of the classical Euler case for a solid with additional degree of freedom - the relative rotation of bodies. Results of the study can be useful for the analysis of dual-spin spacecraft dynamics and for studying the chaotic behavior of the spacecraft.

Index Terms – Axial gyrostat, Andoyer-Deprit variables, solutions in terms of elliptic functions

I. INTRODUCTION

Artificial satellites can contain one or more spinning rotors to provide gyroscopic stability of a desired orientation of the vehicle. Dual-spin spacecraft use the spin of a rotor to maintain pointing accuracy of an antenna platform or a solar sail. Some types of satellites, on the other hand, use small but rapidly spinning momentum wheels to control the attitude of a large platform. In this paper we consider rotational motion of axial dual-spin spacecrafts without external.

The dynamics of a rotating body is a classic topic of study in mechanics. In the eighteenth and nineteenth centuries, several aspects of the motion of a rotating rigid body were studied by such famous mathematicians as Euler, Cauchy, Jacobi, Poinsot, Lagrange and Kovalevskaya. However, the study of the dynamics of rotating bodies is still very important for numerous applications such as the dynamics of satellite-gyrostat, spacecraft, robotics and the like. For example, Rumyantsev [1] developed Lyapunov's ideas arising from the theory of stability of the equilibrium figure of a rotating liquid contained within a gyrostat. The Lyapunov-Rumyantsev theorem is widely used in the design of artificial satellites and liquid-filled projectiles . Andoyer-Deprit canonical variables are used in Hamiltonian structure of an asymmetric gyrostat in the gravitational field[2]. Kinsey et al. [3] focused upon the capture dynamics of the precession phase lock, a phenomenon that could prevent despin of a dual-spin spacecraft by developing a control strategy that employed closed-loop feedback control of the motor torque when the system was near resonance.

Vladimir Aslanov is professor and head of the Theoretical Mechanics Department, Samara State Aerospace University. 34, Moscovskoe shosse, Samara, 443086, Russia (e-mail: aslanov_vs@mail.ru). Manuscript received 10.10.2011; revised 17.10.2011.

Hall [4] proposed a procedure based upon the global analysis of the rotational dynamics. Hall and Rand [5] considered spinup dynamics of classical axial gyrostat composed of an asymmetric platform and an axisymmetric rotor. They obtained averaged equations of motion for slowly varying relative rotation of the bodies (disturbed motion) and analytical solutions in terms of Jacobi’s elliptic functions for the projections of angular momentum in the case of constant relative rotation (undisturbed motion). Anchev [6] derived necessary conditions of stability of permanent rotations of a heavy gyrostat with arbitrary mass distribution and determined the regions of stability on the conical locus formed by the permanent axes. Spinup problems for axisymmetric gyrostats have been investigated by Kane [7]. Elipe [8] investigated a free gyrostat with three flywheels rotating about the three principal axes of inertia and without any external forces or torques. El-Sabaa [9] used Hamiltonian function of the problem of gyrostat is written in terms of Deprit's transform to obtain periodic solutions and the condition for their stability. Recently, many authors have studied different problems of gyrostats in various situations, most of them related to the dynamics of artificial satellites. Some of these authors have received analytical solutions of the equations of motion of free gyrostats [10] or under the influence of a central field [11]. Cochran et al. [10] extended the previous results for axial gyrostats, obtaining solutions for the Euler angles in terms of elliptic integrals. Cavas and Vigueras [11] got solutions for Euler angles in terms of functions of the time. El-Gohary [12-14] studied the control moments sufficient to ensure asymptotic stability of the equilibrium position and rotational motion of a gyrostat, using the Liapunov function. The problem of optimal stabilization of the rotational motion of a symmetrical rigid body with the help of internal rotors is studied by El-Gohary [15]. The control of the angular motion of a rigid body by means of the rotors is studied in Ref. [16]. Tsogas and Kalvouridis and Mavraganis [17] investigated the dynamics of a gyrostat satellite acted upon by the Newtonian forces of N coplanar big bodies, N-1 of which are arranged at equal distances on the periphery of a circle, while the Nth body is located at the mass center of the system; they derived the gyrostat’s equations of motion and its equilibrium states as well as their stability. Kalvouridis [18] studied the dynamics of a small gyrostat satellite acted upon by the Newtonian forces of two big bodies of equal masses which rotate around their center of mass. Balsas and Jimenez and Vera [19] studied two body roto-translatory problems where the rotation of one of them influences strongly in the orbital motion of the system using the canonical action-angle variables. Neishtadt and Pivovarov [20] considered the evolution of the rotation of a gyrostat satellite with slow rotor spinup and worked out formulas for the probabilities which arise due to separatrix crossing. Aslanov [21] obtained explicit analytical time dependences of the Andoyer–Deprit variables corresponding to heteroclinic orbits for all the phase portrait forms of undisturbed motion of axial gyrostats. Although previous works provide insight into the behavior of the axial gyrostats, equations of motion have not been reduced to the system with one degree of freedom and were not found exact analytical solutions for the Andoyer-Deprit canonical variables for the undisturbed motion. Therefore, this paper presents the study of non-linear dynamic behavior of the classical axial gyrostats with zero external torque in the undisturbed. The ratio of the moments of inertia determines the type of gyrostat [Hall]: oblate, prolate and intermediate. The boundary types of the gyrostats (oblate-intermediate and prolate-intermediate) and closely set them cases remain poorly explored. We consider all types of the gyrostats.

This paper is organized as follows. In Section 1, the aim of this paper is formulated. In Section 2, the motion of the axial gyrostats as two rigid bodies connected by a rigid shaft is considered. The gyrostats dynamics is described by ordinary differential equations in the Andoyer-Deprit canonical variables. Section 3 gives the stationary position and their stability. In Section 4, a bifurcation diagram and phase portraits are constructed for gyrostats of all types. The main features of the phase space of the unperturbed system are defined. In Section 5, the general exact analytical solutions for the undisturbed motion of three types of the gyrostats are found in terms of Jacobi's elliptic functions and elementary functions.

II. EQUATIONS OF MOTION

The gyrostat (P+R) consists of the balanced rotor (R), axisymmetric rigid body and the unbalanced platform (P) as shown in Figure 1. The motion differential equations for the angular momentum variables of a rigid axial gyrostat with zero external torque may be written as [22]

$$\frac{dh_1}{dt} = \frac{I_2 - I_3}{I_2 I_3} h_2 h_3 , \tag{1}$$

$$\frac{dh_2}{dt} = \left(\frac{I_3 - I_P}{I_3} h_1 - h_a \right) \frac{h_3}{I_P} , \tag{2}$$

$$\frac{dh_3}{dt} = \left(\frac{I_P - I_2}{I_2} h_1 + h_a \right) \frac{h_2}{I_P} \tag{3}$$

where e_i are principal axes of $P+R$ ($i = 1,2,3$), $h_a = I_S(\omega_S + \omega_1) = const$ is a angular momentum of R about e_1, $h_1 = I_1\omega_1 + I_S\omega_S$ is a angular momentum of $P+R$ about e_1, $h_i = I_i\omega_i$ are angular momentums of $P+R$ about e_i ($i = 2,3$), I_i are moments of inertia of $P+R$ about e_i ($i = 1,2,3$), $I_P = I_1 - I_S$ is a moment of inertia of P about e_1, I_S is moment of inertia of R about e_1, t is time, ω_i are angular velocities of P about e_i ($i = 1,2,3$), ω_S is a angular velocity of R about e_1 relative to P.

Since external moments, angular momentum are conserved, the first integral of the motion is

$$G = \sqrt{h_1^2 + h_2^2 + h_3^2} = const \tag{4}$$

This first integral allows us to reduce the number of equations (1)-(3) by one. However it gives complicated equations of the motion. The equations of motion can be simplified by using the canonical Andoyer-Deprit variables [23,24]: l, g, h, L, G, H . In our case the first integral (4) is included directly in the Andoyer-Deprit variables. Using the change of variables

$$h_1 = L, \quad h_2 = \sqrt{G^2 - L^2}\sin l, \quad h_3 = \sqrt{G^2 - L^2}\cos l \tag{5}$$

we obtain the equations of motion in terms of Andoyer–Deprit variables

$$\dot{l} = \frac{1}{I_P}\left[L - h_a - \frac{1}{2}L\left(a + b + (b-a)\cos 2l\right)\right], \tag{6}$$

$$\dot{L} = \frac{1}{2I_P}(b-a)\left(G^2 - L^2\right)\sin 2l \tag{7}$$

where $\dot{x} = dx/dt$, $a = I_P / I_2$, $b = I_P / I_3$. The body axes have been chosen so that $I_2 > I_3$ (or equivalently $b > a$).

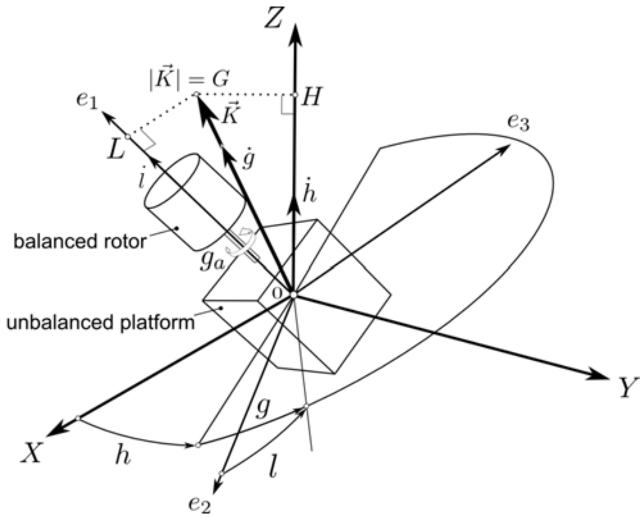

FIGURE 1. The axial gyrostat

The transformation of equations (6) – (7) to dimensionless form is obtained by scaling two momentum, time and axial torque as follows

$$s = \frac{L}{G},\ d = \frac{h_a}{G},\ \tau = t\frac{G}{I_p} \tag{8}$$

Derivatives with respect to τ are denoted by a derivative sign: $x' = dx/d\tau$. Carrying out change of variables (8) leads to the equivalent set of canonical equations

$$l' = \frac{\partial H}{\partial s} = s - d - \frac{s}{2}\left[(a+b) + (b-a)\cos 2l\right], \tag{9}$$

$$s' = -\frac{\partial H}{\partial l} = \frac{1}{2}(b-a)\left(1 - s^2\right)\sin 2l \tag{10}$$

where H is a Hamiltonian

$$H(l,s) = \frac{1-s^2}{4}\left[(a+b) + (b-a)\cos 2l\right] + \frac{s^2}{2} - sd = h = const \tag{11}$$

Solving the expression (11) with respect to the $\cos 2l$ we obtain an equation of the phase trajectory

$$\cos 2l = \frac{(a+b-2)s^2 + 4ds + 4h - a - b}{(1-s^2)(b-a)} \quad (12)$$

III. STATIONARY SOLUTIONS

We define stationary solutions of equations (9) and (10). Equating to zero these equations leads to four stationary solutions. The first and second stationary solutions are described by, respectively

$$\cos(2l_*) = 1,\ s_* = \frac{d}{1-b}, \quad (13)$$

$$\cos(2l_*) = -1,\ s_* = \frac{d}{1-a} \quad (14)$$

The third and fourth stationary solutions correspond to the cases when axis of rotation gyrostat e_1 coincides with the angular momentum, or takes the opposite direction

$$\cos(2l_*) = \frac{2-a-b-2d}{b-a}, \qquad s_* = 1 \quad (15)$$

$$\cos(2l_*) = \frac{2-a-b+2d}{b-a}, \qquad s_* = -1 \quad (16)$$

We will perform the standard procedure of linearization (9) and (10) in the vicinity of a stationary position $\Delta l = l_* - l,\ \Delta s = s_* - s$, then a characteristic equation can be written as

$$\begin{vmatrix} \frac{\partial^2 H}{\partial s \partial l} - \lambda & \frac{\partial^2 H}{\partial s^2} \\ -\frac{\partial^2 H}{\partial l^2} & -\frac{\partial^2 H}{\partial l \partial s} - \lambda \end{vmatrix} = 0 \quad (17)$$

This characteristic equation for first stationary solution (13) becomes

$$\lambda^2 - (b-a)(1-b)(1-s_*^2) = 0$$

The equilibrium position (13) is obviously stable if

$$b > 1 \ \ (I_P > I_3) \quad (18)$$

and unstable if

$$b < 1 \ \ (I_P < I_3) \quad (19)$$

For the second stationary solution (14), the characteristic equation (17) can be written as

$$\lambda^2 - (b-a)(a-1)(1-s_*^2) = 0$$

then the second stationary solution (19) will be stable if

$$a < 1 \ \ (I_P < I_2) \quad (20)$$

and unstable for

$$a > 1 \ \ (I_P > I_2) \quad (21)$$

Thus, the equilibrium position $l_* = n\pi, n \in \mathbb{Z}$ is stable, if the moment of inertia of the platform I_P greater than the smaller moments of inertia of gyrostat I_2 and unstable, if I_P less than I_2. The equilibrium position $l_* = \pi/2 + \pi n,\ n \in \mathbb{Z}$ is stable if the moment of inertia of the platform is less than the larger of the transverse moments of inertia gyrostat and unstable if more than that moment of inertia.

For the third and fourth stationary solutions (15) and (16), the characteristic equation (17) can be written as

$$\lambda^2 - (b-a)^2 (1 - \cos^2 2l_*) = 0$$

This equation has only real roots, so the third and fourth stationary solutions (15) and (16) are unstable.

IV. BIFURCATION DIAGRAM

Depending on the ratio of moments of inertia we distinguish between five types of gyrostats:

1) Oblate Gyrostat: $I_p > I_2 > I_3 \ (b > a > 1)$,
2) Oblate-Intermediate Gyrostat: $I_p = I_2 > I_3 \ (b > a = 1)$,
3) Intermediate Gyrostat: $I_2 > I_p > I_3 \ (b > 1 > a)$,
4) Prolate-Intermediate Gyrostat: $I_2 > I_p = I_3 \ (b = 1 > a)$,
5) Prolate Gyrostat: $I_2 > I_3 > I_p \ (1 > b > a)$.

Gyrostats 1), 3) and 5) correspond to areas with the same numbers in Figure 2, gyrostat 2) corresponds to the border between areas 1 and 3 and type 4) – to the border between areas 3 and 5.

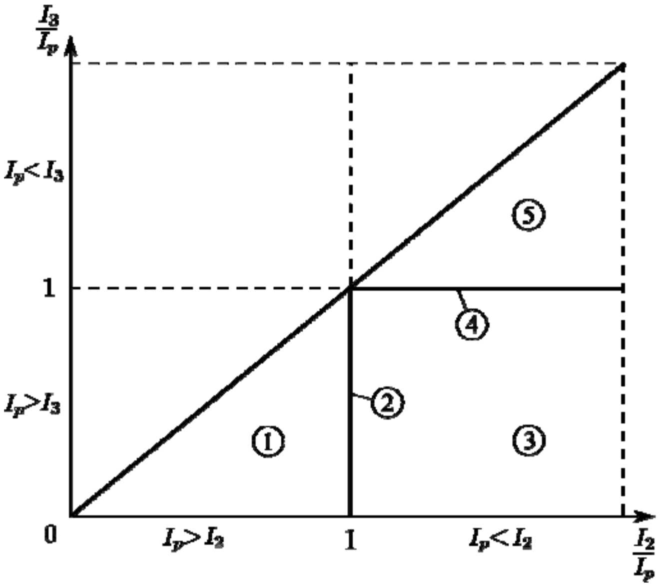

FIGURE 2. The bifurcation diagram

The coordinates critical points for all types of the gyrostats given in Table 1, where the subscripts "c" and "s" denote centers and saddles, respectively. The coordinates of the critical points correspond to stationary solutions obtained above (13)-(16).

TABLE 1

The critical points coordinate for various types of gyrostats

Case	Gyrostat type	The critical points	The additional conditions
1a	Oblate $I_p > I_2 > I_3$ $(b > a > 1)$	$l_c = 0$ $s_c = d/(1-b)$ $l_s = \pi/2$ $s_s = d/(1-a)$	$\left\lvert \frac{d}{1-a} \right\rvert < 1$
1b		$l_c = 0$	$\left\lvert \frac{d}{1-a} \right\rvert \geq 1$

Case	Gyrostat type	The critical points	The additional conditions
		$s_c = d/(1-b)$ $\cos 2l_s = \dfrac{2-a-b+2d}{b-a}$ $s_s = -\operatorname{sgn} d$	
2	Oblate-Intermediate $I_p = I_2 > I_3$ $(b > a = 1)$	$l_c = 0$ $s_c = d/(1-b)$ $\cos 2l_s = \dfrac{2-a-b+2d}{b-a}$ $s_s = -\operatorname{sgn} d$	$\left\lvert \dfrac{d}{1-a} \right\rvert \to \infty$
3a	Intermediate $I_2 > I_p > I_3$ $(b > 1 > a)$	$l_c = 0$ $s_c = d/(1-b)$ $\cos 2l_s = \dfrac{2-a-b+2d}{b-a}$ $s_s = -\operatorname{sgn} d$	$\left\lvert \dfrac{d}{1-a} \right\rvert \ge 1$
3b		$l_c = 0$ $s_c = d/(1-b)$ $\cos 2l_s = \dfrac{2-a-b+2d}{b-a}$ $s_s = -\operatorname{sgn} d$	$\left\lvert \dfrac{d}{1-a} \right\rvert < 1$
		$l_c = \pi/2$ $s_c = d/(1-a)$ $\cos 2l_s = \dfrac{2-a-b-2d}{b-a}$ $s_s = \operatorname{sgn} d$	$\left\lvert \dfrac{d}{1-b} \right\rvert < 1$
3c		$l_c = \pi/2$ $s_c = d/(1-a)$ $\cos 2l_s = \dfrac{2-a-b-2d}{b-a}$ $s_s = \operatorname{sgn} d$	$\left\lvert \dfrac{d}{1-b} \right\rvert \ge 1$
4	Prolate-Intermediate $I_2 > I_p = I_3$ $(b = 1 > a)$	$l_c = \pi/2$ $s_c = d/(1-a)$ $\cos 2l_s = \dfrac{2-a-b-2d}{b-a}$ $s_s = \operatorname{sgn} d$	$\left\lvert \dfrac{d}{1-b} \right\rvert \to \infty$
5a	Prolate $I_2 > I_3 > I_p$ $(1 > b > a)$	$l_c = \pi/2$ $s_c = d/(1-a)$ $\cos 2l_s = \dfrac{2-a-b-2d}{b-a}$ $s_s = \operatorname{sgn} d$	$\left\lvert \dfrac{d}{1-b} \right\rvert \ge 1$
5b		$l_c = \pi/2$ $s_c = d/(1-a)$ $l_s = 0$ $s_s = d/(1-b)$	$\left\lvert \dfrac{d}{1-b} \right\rvert < 1$

First, consider cases 1a, 3b and 5b where the absolute value of momentum s is less than unity ($|s| < 1$). Examples of phase trajectories for the Oblate Gyrostat (1a), the Prolate Gyrostat (5b) and the Intermediate Gyrostat (3b) are shown in s, l coordinates in Figure 3-5. In Figure 5, there are two types of separatrix for the Intermediate Gyrostat (3b), one of which contains saddles with s_s=-sgn d and another saddle width s_s=sgn d (29). In the phase space bounded by these separatrixes, there is continuous motion with sequential change in the sign of the momentum s.

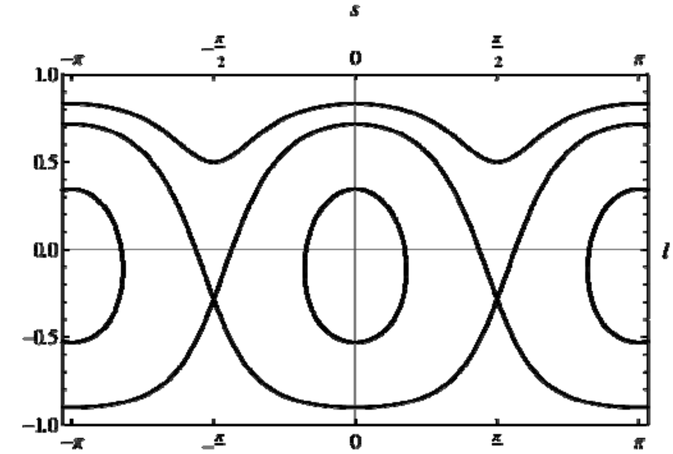

FIGURE 3. Phase trajectories for the Oblate Gyrostat (1a): $I_2 = 0.85\,kg\,m^2$, $I_3 = 0.65\,kg\,m^2$, $I_p = 1.0\,kg\,m^2$, $d = 0.05$, $\left[s_c = -0.093(l_c = 0),\ s_s = -0.283(l_s = \pm\pi/2)\right]$

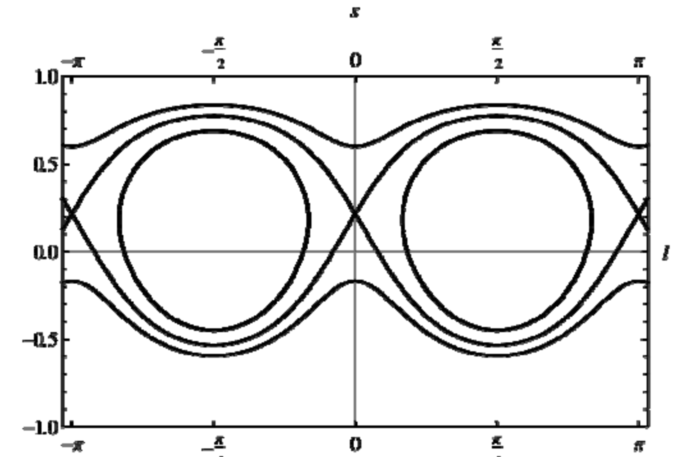

FIGURE 4. Phase trajectories for the Prolate Gyrostat (5b): $I_2 = 0.85\,kg\,m^2$, $I_3 = 0.65\,kg\,m^2$, $I_p = 0.5\,kg\,m^2$, $d = 0.05$, $\left[s_c = 0.2125(l_s = \pm\pi/2),\ s_s = 0.2167(l_c = 0)\right]$

According to Table 1 the saddles are located on the horizontals $s = \pm 1$ in all other cases. In the case of 1b, 2 and 3a – on the horizontal $s_s = -\operatorname{sgn} d$, and in the cases of 3c, 4 and 5a – on the horizontal $s_s = \operatorname{sgn} d$. Examples of phase trajectories for the Oblate-Intermediate Gyrostat (2) and the Prolate-Intermediate Gyrostat (4) are shown in s, l coordinates in Figure 6-7.

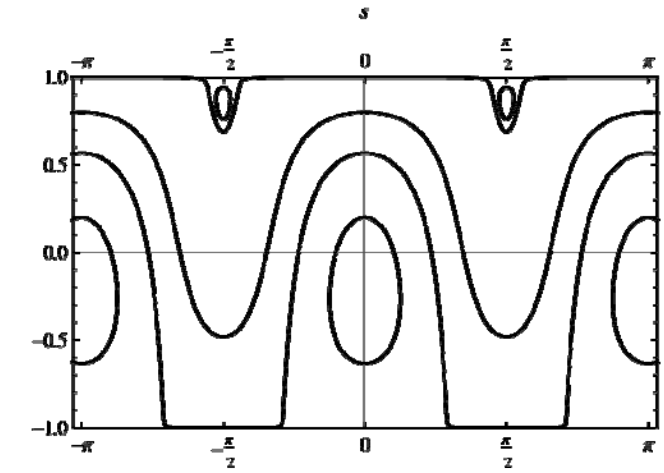

FIGURE 5. Phase trajectories for the Intermediate Gyrostat (3b): $I_2 = 0.85\,kg\,m^2$, $I_3 = 0.65\,kg\,m^2$, $d = 0.05$.
Centers: $\left[s_c = -0.2167\left(l_s = 0\right),\ s_c = 0.85\left(l_c = \pm\pi/2\right)\right]$.
Saddles: $\left[s_s = 1.0\left(l_s = \pm 1.3953\right),\ s_s = -1.0\left(l_s = \pm 0.9109\right)\right]$

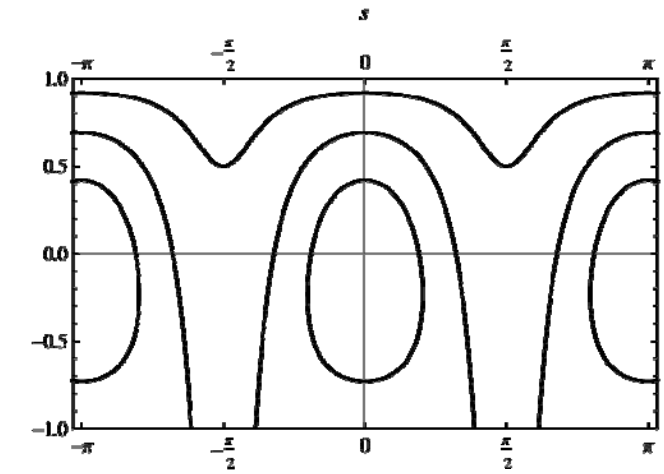

FIGURE 6. Phase trajectories for the Oblate-Intermediate Gyrostat (2): $I_p = I_2 = 0.85\,kg\,m^2$, $I_3 = 0.65\,kg\,m^2$, $d = 0.05$
$\left[s_c = -0.1625\ \left(l_c = 0\right),\ \ s_s = -1\left(l_s = \pm 1.15588\right)\right]$

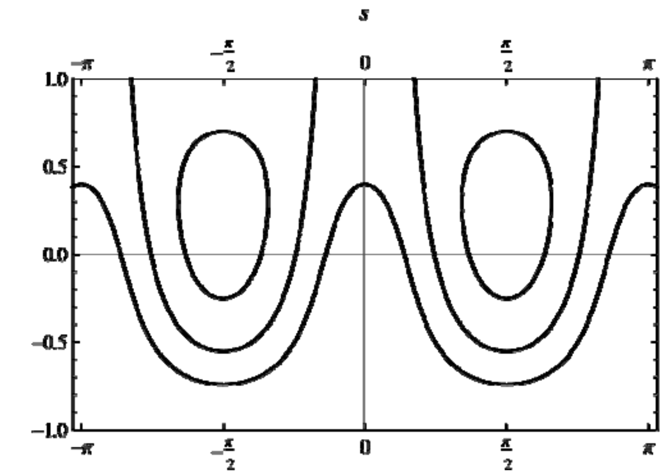

FIGURE 7. Phase trajectories for the Prolate-Intermediate Gyrostat (4): $I_2 = 0.85\,kg\,m^2$, $I_p = I_3 = 0.65\,kg\,m^2$, $d = 0.05$, $I_p = 0.8\,kg\,m^2$,
$[s_c = 0.2125, \left(l_c = \pm\pi/2\right)\ s_c = 1\ \left(l_c = \pm 0.4791\right)]$

V. INTEGRATION BY QUADRATURE THE EQUTIONS OF UNDISTURBED MOTION

A. Separation of variables

In this paper we'll find the analytic solutions of canonical equations (9) and (10) only for the case when the momentum $|s| < 1$. According to Table 1, this condition corresponds to the following types gyrostats: oblate (1a), prolate (5b) and intermediate (3b).

By deleting the coordinate l from the equation (10) and making use of equation (12), we obtain the new form

$$s' = \pm\frac{1}{2}\sqrt{\left[\left(1-s^2\right)\left(b-a\right)\right]^2 - \left[\left(a+b-2\right)s^2 + 4ds + 4h - a - b\right]^2}$$
$$= \pm\sqrt{F(s)} \qquad (22)$$

where

$$F(s) = -4\,f_a(s)\,f_b(s) \qquad (23)$$

$$f_\gamma(s) = \frac{1}{2}\left(1-\gamma\right)s^2 - ds + \frac{\gamma}{2} - h, \left(\gamma = a, b\right) \qquad (24)$$

Separating the variables in the equation (35) and integrating it we obtain

$$\tau = \pm\int\frac{ds}{\sqrt{F(s)}} + const \qquad (25)$$

In a general case, this integral is an elliptic integral. Transform the integral to the Legendre normal form [25] depends on the type and location of the roots of the fourth-degree polynomial (23) as the product of two polynomials of second degree (24). We represent the roots of the quadratic equations

$$f_\gamma(s) = 0\ \left(\gamma = a, b\right)$$

as

$$s_{1,2}^{\gamma} = \frac{d \pm \sqrt{D_\gamma}}{1-\gamma},\ D_\gamma = d^2 + \left(2h-\gamma\right)\left(1-\gamma\right) \qquad (26)$$

B. Analytical solutions for the oblate gyrostat

The type of the roots (26) of the polynomial (23) depends on the h constant. For different types of the motion of the oblate gyrostat $\left(b > a > 1\right)$ h corresponds to the following condition

$$h_c > h_L > h_s > h_R \qquad (27)$$

where h_L and h_R are correspond to libration and rotation respectively. The constant h in the center – h_c and in the saddle – h_s is

$$h_c = \frac{1}{2}\left(b - \frac{d^2}{1-b}\right),\ h_s = \frac{1}{2}\left(a - \frac{d^2}{1-a}\right) \qquad (28)$$

We have libration's solution if an arbitrary constant $h = h_L$ satisfy condition (27), and then the phase trajectory belongs to the closed area (Fig. 3), which includes the center $l_c = 0 \pm \pi k, k \in \mathbb{Z}$, $s_c = d/\left(1-b\right)$. The roots of the polynomial (31) with (34) are given by

$$s_{1,2} = s_{1,2}^b = \frac{d \mp \sqrt{D_b}}{1-b},$$
$$D_b = d^2 + (2h_L - b)(1-b) > 0$$
$$s_{3,4} = s_{1,2}^a = s_s \pm is_k, s_k = \frac{\sqrt{-D_a}}{1-a},$$
$$D_a = d^2 + (2h_L - a)(1-a) < 0$$

Two real roots $s_1 > s_2$ and two complex conjugate roots $s_{3,4} = s_s \pm is_k$ take place because the integral (25) can be written as

$$\lambda\tau = \int_{s_2}^{s} \frac{ds}{\sqrt{(s_1 - s)(s - s_2)(s - s_3)(s - s_4)}} \quad (29)$$

The change of variable [9]

$$\left(\tan\frac{\varphi}{2}\right)^2 = \frac{\cos\theta_1}{\cos\theta_2}\frac{s_1 - s}{s - s_2} \quad (30)$$

converts the integral (29) to the Legendre normal form

$$\omega\tau = \int_{\pi}^{\varphi} \frac{d\varphi}{\sqrt{1 - k^2 \sin^2\varphi}}$$

where

$\tan\theta_1 = \frac{s_1 - s_s}{s_k}$, $\tan\theta_2 = \frac{s_2 - s_s}{s_k}$ (θ_1, θ_2 are acute angles),

$$\omega = \frac{\lambda}{\mu},\ k = \frac{\sin\theta_1 - \sin\theta_2}{2},\ \mu = -\frac{(\cos\theta_1\cos\theta_2)^{1/2}}{s_k}$$

We proceed to study the rotation when $h = h_R$ in the condition (27). The four real roots of the equation $F(s) = 0$ take place: two roots $(s_2 < s < s_1)$ correspond to the upper phase trajectories and two roots $(s_4 < s < s_3)$ the lower phase trajectories as shown in Fig. 3.

$$s_{3,2} = s_{1,2}^a = \frac{d \pm \sqrt{D_a}}{1-a},\ D_a = d^2 + (2h_R - a)(1-a) > 0$$
$$s_{4,1} = s_{1,2}^b = \frac{d \pm \sqrt{D_b}}{1-b},\quad D_b = d^2 + (2h_R - b)(1-b) > 0$$

Since $D_a < D_b$ then the real roots are as follows

$$-1 < s_4 < s_3 < s_2 < s_1 < 1 \quad (31)$$

In this case the integral (25) has the form

$$\lambda\tau = \int_{s_i}^{s} \frac{ds}{\sqrt{(s_1 - s)(s - s_2)(s - s_3)(s - s_4)}} \quad (32)$$

where index of the lower limit of the integral $i = 2$ for the upper phase trajectories and $i = 4$ for the lower phase trajectories. By the change of variables [25] the integral (32) can be reduced to the Legendre normal integral

$$\omega\tau = \int_0^{\varphi} \frac{d\varphi}{\sqrt{1 - k^2 \sin^2\varphi}} \quad (33)$$

Then the general solutions can be written for the upper area $(s_2 < s < s_1)$

$$s = \frac{s_2 s_{31} - s_3 s_{21} sn^2(\omega\tau, k)}{s_{31} - s_{21} sn^2(\omega\tau, k)} \quad (34)$$

and for the low area $(s_4 < s < s_3)$

$$s = \frac{s_4 s_{31} + s_1 s_{43} sn^2(\omega\tau, k)}{s_{31} + s_{41} sn^2(\omega\tau, k)} \quad (35)$$

where $sn(\omega\tau, k)$ is a elliptic sine

$$\omega = \frac{\lambda}{\mu},$$
$$k^2 = \frac{(s_3 - s_4)(s_2 - s_1)}{(s_3 - s_1)(s_2 - s_4)},\ \mu = 2(s_{31}s_{24})^{-1/2},\ s_{ij} = s_j - s_i$$

C. Analytical solutions for the prolate gyrostat

For the prolate gyrostat the constant h satisfies the following condition for different types of motion

$$0 < h_c < h_L < h_s < h_R \quad (36)$$

where

$$h_c = \frac{1}{2}\left(a - \frac{d^2}{1-a}\right), h_s = \frac{1}{2}\left(b - \frac{d^2}{1-b}\right) \quad (37)$$

There is a libration, when arbitrary constant $h = h_L$ satisfies to condition (44). The roots (26) of polynomial (23) are written by

$$s_{1,2} = s_{1,2}^a = \frac{d \pm \sqrt{D_a}}{1-a},$$
$$D_a = d^2 + (2h_L - a)(1-a) > 0,$$
$$s_{3,4} = s_{1,2}^b = s_s \pm is_k,\ s_k = \frac{\sqrt{-D_b}}{1-b},$$
$$D_b = d^2 + (2h_L - b)(1-b) < 0$$

From this is clear that desired solutions coincide with the solutions (30). In the case of rotation of the prolate gyrostat there are four real roots (26)

$$s_{1,4} = s_{1,2}^a = \frac{d \pm \sqrt{D_a}}{1-a},\ D_a = d^2 + (2h_R - a)(1-a) > 0$$
$$s_{2,3} = s_{1,2}^b = \frac{d \pm \sqrt{D_b}}{1-b},\quad D_b = d^2 + (2h_R - b)(1-b) > 0$$

The location of these real roots

$$-1 < s_4 < s_3 < s_2 < s_1 < 1$$

coincide with the location of the roots (31). Therefore, in this case the general solutions are the solutions (34) and (35).

D. Analytical solutions for the intermediate gyrostat

The moments of inertia of the intermediate gyrostat determined by the following relation $I_3 < I_p < I_2$, $(b < 1 < a)$. In this case we have two groups of libration areas, when the phase trajectories are closed: 0-areas, which includes centers,

$$l_c = 0 \pm \pi k, k \in \mathbb{Z},\ s_c = d/(1-b)$$

and 1-areas containing centers

$$l_c = \pi/2 \pm \pi k,\ k \in \mathbb{Z},\ s_c = d/(1-a)$$

These areas correspond to values of the arbitrary constant of the Hamiltonian h_{L0} и h_{L1}. As shown in Fig. 5 the phase portrait has a single area of rotations and opened trajectories, in which $h = h_R$. The constant h for the different types of motion corresponds to the following condition:

$$0 < h_{c1} < h_{L1} < h_{s1} < h_R < h_{s0} < h_{L0} < h_{c0} \quad (38)$$

where h_{c0} and h_{s0} correspond respectively to the centers with $l_c = 0 \pm \pi k, k \in \mathbb{Z}$ and the saddles with $s_s = -\operatorname{sgn} d$ (row 3b in Table 1)

$$h_{c0} = \frac{1}{2}\left(b - \frac{d^2}{1-b}\right),\ h_{s0} = \frac{1}{2} + d \quad (39)$$

h_{c1} and h_{s1} correspond to the centers with $l_c = \pi/2 \pm \pi k,\ k \in \mathbb{Z}$ and the saddles with $s_s = \operatorname{sgn} d$

$$h_{c1} = \frac{1}{2}\left(a - \frac{d^2}{1-a}\right), h_{s1} = \frac{1}{2} - d \quad (40)$$

For the librations in the 0-areas ($h = h_{L0}$), which includes centers $l_c = 0 \pm \pi k, k \in \mathbb{Z}$, we have the following roots of the polynomial (23)

$$s_{1,4} = s_{1,2}^a = \frac{d \pm \sqrt{D_{a0}}}{1-a}, D_{a0} = d^2 + (2h_{L0} - a)(1-a) > 0 \quad (41)$$

$$s_{3,2} = s_{1,2}^b = \frac{d \pm \sqrt{D_{b0}}}{1-b}, D_{b0} = d^2 + (2h_{L0} - b)(1-b) > 0 \quad (42)$$

For the 1-areas ($h = h_{L1}$), which includes centers $l_c = \pi/2 \pm \pi k,\ k \in \mathbb{Z}$, the roots of the polynomial (23) are

$$s_{4,3} = s_{1,2}^a = \frac{d \pm \sqrt{D_{a1}}}{1-a}, D_{a1} = d^2 + (2h_{L1} - a)(1-a) > 0, \quad (43)$$

$$s_{2,1} = s_{1,2}^b = \frac{d \pm \sqrt{D_{b1}}}{1-b}, D_{b1} = d^2 + (2h_{L1} - b)(1-b) > 0 \quad (44)$$

The numbering of the roots of (41)-(44) corresponds to the following sequence

$$s_4 < -1 < s_3 < s_2 < 1 < s_1 \quad (45)$$

Physical motion is realized in the range $s \in (s_3, s_2)$. In this case the integral (25) becomes

$$\lambda\tau = \int_{s_3}^{s} \frac{ds}{\sqrt{(s-s_1)(s-s_2)(s-s_3)(s-s_4)}} \quad (46)$$

where $\lambda = \sqrt{(A_\Sigma - C)(C - B_\Sigma)/(A_\Sigma B_\Sigma)}$.

The elliptic integral (46) reduces to the Legendre normal form (33) with the following change of variables [9]

$$s = \frac{s_3 s_{42} - s_4 s_{32} \sin^2\varphi}{s_{42} - s_{32}\sin^2\varphi}$$

where

$$\omega = \frac{\lambda}{\mu},\ k^2 = \frac{(s_1 - s_4)(s_2 - s_3)}{(s_1 - s_3)(s_2 - s_4)},$$

$$\mu = 2(s_{31}s_{42})^{-1/2}, s_{ij} = s_j - s_i$$

Then the general solutions can be written as

$$s = \frac{s_3 s_{42} - s_4 s_{32}\, sn^2(\omega\tau, k)}{s_{42} - s_{32}\, sn^2(\omega\tau, k)} \quad (47)$$

We consider the area of rotation (Fig. 5), bounded by 0- and 1-separatrices. Range of variation of arbitrary constant $h_R \in (h_{s1}, h_{s0})$ or, according to (39) and (40)

$$h_R \in \left(\frac{1}{2} - d, \frac{1}{2} + d\right)$$

Then the four roots (26) have the form

$$s_{4,3} = s_{1,2}^a = \frac{d \pm \sqrt{D_a}}{1-a},\ D_a = d^2 + (2h_R - a)(1-a) > 0 \quad (48)$$

$$s_{2,1} = s_{1,2}^b = \frac{d \pm \sqrt{D_b}}{1-b},\quad D_b = d^2 + (2h_R - b)(1-b) > 0 \quad (49)$$

Physical motion is realized in the range $s \in (s_3, s_2)$. The location of the roots (48) and (49) corresponds to (45), therefore the solution (47) describes also the rotation of the intermediate gyrostat.

VI. CONCLUSION

We have shown that the equations of motion for the axial gyrostats can be reduced to two first-order ordinary differential equations for the Andoyer-Deprit canonical variables. The stationary solutions are found and studied their stability. Also we obtain the general exact analytical solutions in terms of elliptic functions. Note that an analytical description of the motion along the separatrix is easily obtained. It's enough to substitute $sn(u,1) = \tanh(u)$ in the founded solutions for the libration or the rotation. These results can be interpreted as the development of the classical Euler case for a solid, when added one degree of freedom - the relative rotation of bodies. Results of the study can be useful for the analysis of dual-spin spacecraft dynamics and for studying the chaotic behavior of the spacecraft.

ACKNOWLEDGEMENT

This research was supported by the Russian Foundation for Basic Research (09-01-00384).

REFERENCES

[1] Rumyantsev V.V.: On the Lyapunov's methods in the study of stability of motions of rigid bodies with fluid-filled cavities, Adv. Appl. Mech. 8, 183-232 (1964)

[2] Tong X., Tabarrok B., Rimrott F.: Chaotic motion of an asymmetric gyrostat in the gravitational field, Int. J. Non-Linear Mech. 30, 191-203 (1995)

[3] Kinsey K.J., Mingori D.L., Rand R.H.: Non-linear control of dual-spin spacecraft during despin through precession phase lock, J. Guidance Control Dyn. 19, 60-67 (1996)

[4] Hall C.D.: Escape from gyrostat trap states, J. Guidance Control Dyn. 21, 421-426 (1998)

[5] Hall, C. D., and Rand, R. H.: "Spinup Dynamics of Axial Dual-Spin Spacecraft," Journal of Guidance, Control, and Dynamics, 17, n. 1, 30-37 (1994).

[6] Anchev, A.: On the stability of the permanent rotations of a heavy gyrostat. J. of Applied Mathematics and Mechanics, 26, n 1, 22-28 (1962).

[7] Kane,T.R.: Solution of the Equations of rotational motion for a class of torque-free gyrostats. AIAA Journal, 8, n 6, 1141-1143 (1970).

[8] Elipe, A.: Gyrostats in free rotation. IAU Colloquium, 165, 1-8 (1991).

[9] El-Sabaa, F.M.: Periodic solutions and their stability for the problem of gyrostat. Astrophysics and Space Science, 183, 199-213 (1991).

[10] Cochran, J. E., Shu, P.-H., and Rew, S. D.: Attitude Motion of Asymmetric Dual-Spin Spacecraft, Journal of Guidance, Control, and Dynamics, 5, n 1, 37-42 (1982).

[11] Cavas, J.A., Vigueras,A.: An integrable case of rotational motion analogue to that of Lagrange and Poisson for a gyrostat in a Newtonian force field, Cel.Mech.Dynam.Astron., 60, 317-330 (1994).

[12] El-Gohary, A. I.: On the stability of an equilibrium position and rotational motion of a gyrostat, Mech. Res. Comm., 24, 457-462 (1997).

[13] El-Gohary A.: On the control of programmed motion of a rigid containing moving masses, Int. J. Non-Linear Mech, 35, n 1, 27-35(2000).

[14] El-Gohary A.: On the stability of the relative programmed motion of a satellite gyrostat, Mechanics Research Communications, 25, n 4, 371-9 (1998).

[15] El-Gohary A.: Optimal stabilization of the rotational motion of rigid body with the help of rotors, Int. J. Non-Linear Mech., 35, n 3, 393-403 (2000).

[16] El-Gohary, A., Hassan, S.Z.: On the exponential stability of the permanent rotational motion of a gyrostat, Mechanics Research Communications, 26, n 4, 479-488 (1999).

[17] Tsogas, V., Kalvouridis, T.J., Mavraganis, A.G.: Equilibrium states of a gyrostat satellite moving in the gravitational field of an annular configuration of N big bodies, Acta Mechanica, 175, n 1-4, 181-195 (2005).

[18] Kalvouridis, T.J.: Stationary solutions of a small gyrostat in the Newtonian field of two massive bodies, Nonlinear Dynamics, 61, n 3, 373-381 (2010).

[19] Balsas, M.C., Jimenez, E.S., Vera, J.A.: The motion of a gyrostat in a central gravitational field: phase portraits of an integrable case, J. Nonlinear Math.Phys.,15, 53-64 (2008).

[20] Neishtadt A.I., Pivovarov M.L.: Separatrix crossing in the dynamics of a dual-spin satellite, J. of Applied Mathematics and Mechanics, 64, 741-746 (2000).

[21] Aslanov V., Behavior of Axial Dual-spin Spacecraft, Lecture Notes in Engineering and Computer Science: Proceedings of The World Congress on Engineering 2011, WCE 2011, 6-8 July, 2011, London, U.K., pp 13-18.

[22] Hughes, P.C.: Spacecraft Attitude Dynamics, Wiley, New York (1986).

[23] Andoyer H.: Cours de Mechanique Celeste, Vol. 1, Gauthier-Villars (1923).

[24] Deprit A.: A free rotation of a rigid body studied in the phase plane, American Journal of Physics, 35 , 424 – 428 (1967)

[25] Korn G., Korn T.: Mathematical handbook, McGraw-Hill Book Company, New York (1968).